

Article

Rescaled Statistics and Wavelet Analysis on Agricultural Drought Disaster Periodic Fluctuations in China from 1950 to 2016

Qian Wang, Yangyang Liu, Linjing Tong, Weihong Zhou, Xiaoyu Li and Jianlong Li *

Department of Ecology, School of Life Sciences, Nanjing University, Nanjing 210093, China; dg1730046@smail.nju.edu.cn (Q.W.); dg1730043@smail.nju.edu.cn (Y.L.); mg1730074@smail.nju.edu.cn (L.T.); zhouweihong07@lzu.edu.cn (W.Z.); mg1730069@smail.nju.edu.cn (X.L.)

* Correspondence: jlli2008@nju.edu.cn; Tel.: +86-025-8621-4644

Received: 18 July 2018; Accepted: 5 September 2018; Published: 12 September 2018



Abstract: An agricultural drought disaster was analyzed with the new insight of rescaled statistics (R/S) and wavelet analysis in this study. The results showed that: (1) the Hurst index of the agricultural disaster area, the inundated area of agricultural drought disaster, and the grain loss was 0.821, 0.874, and 0.953, respectively, indicating that the process of the agricultural drought disaster had stronger positive continuity during the study period; (2) based on the Morlet analysis of the agricultural disaster area, the inundated area of the agricultural drought disaster, and the grain loss of China from 1950 to 2016, the time series of the agricultural drought had multiple time scale features with the periodic variation on a large scale containing the periodic variation on a small scale; and (3) in the last 67 years, the strong wavelet energy spectrum of the agricultural disaster area, the inundated area of the agricultural drought disaster, and the grain loss was at the time scale of ≈ 22 –32 years, ≈ 24 –32 years, and ≈ 25 –32 years, respectively. In addition, the first major period in the agricultural drought disaster area, the inundated area of agricultural drought disaster, and the grain loss had average periods of approximately 16 years, 16 years, and 18 years, respectively.

Keywords: R/S; Morlet analysis; agricultural drought disaster; periodic oscillation

1. Introduction

Drought is one of the most serious meteorological disasters because of its high frequency, long duration, and wide range of effects [1]. Generally, there are four types of drought: meteorological, agricultural, hydrological, and socio-economic drought [2,3]. According to the World Meteorological Organization, as many as 55 drought indices are in common use to monitor and evaluate the different types of droughts [4]. For example, the standardized precipitation evapotranspiration index (SPEI), soil moisture anomaly percentage index (SMAPI), and standardized runoff index (SRI) are used to describe meteorological, agricultural, and hydrological droughts, respectively [5]. Recent studies indicate that severe drought with more frequency and persistent duration may be somewhat due to the increasing intensity of global warming [6]. Drought disaster as a recurring extreme climate event plays an important part for agriculture and causes huge grain loss all over the world [7]. In addition, drought disaster also has caused a serious effect on the food security, water resource, and energy recycles.

Therefore, much focus has been put into drought scenarios in recent years. Some scholars study the relationships between drought and precipitation, climate, and other factors, suggesting the mechanism of drought, and others analyzed the spatial and temporal characteristics of droughts using the drought index, indicating the drought distribution and the severity level [8]. However, what will be the trend of the agricultural drought disaster in the future? What is the periodic oscillation of agricultural drought

disasters? In this study, we attempt to answer these questions using the new insight of rescaled statistics (R/S) and wavelet analysis.

Hurst's rescaled range is to provide an assessment of how the apparent variability of a series changes with the length of the time-period being considered [9]. Furthermore, it has been applied to many research fields. Since it is robust with few assumptions about the underlying system, it has broad applicability for time series analysis [10]. For droughts, which are long-lasting natural disasters with widespread impacts, R/S is a suitable tool for forecasting the trend of droughts.

The wavelet transform is a mathematical tool that provides a time scale representation of a signal in the time domain [11] and is usually used to identify the location of the mutation point in non-stationary signals [12]. It has been used to assess the processes of hydrology and meteorology [13,14]. Furthermore, droughts are caused by less precipitation and higher temperatures over time. Because drought is typically a non-stationary process, wavelet transform (WT) is a suitable tool for managing drought data.

China as an agricultural country is a typical monsoon climate country with an agricultural drought disaster. During the last decade, the severe drought in southwest China has resulted in tremendous losses, including crop failure, a lack of drinking water, and ecosystem destruction [15]. Therefore, drought has become the key obstacle factor constraining China's agriculture and sustainable development. Numerous studies have been conducted in the field of drought risk assessment in China. Li (2004) established the risk evaluation system of disasters related to drought and winter wheat in northern China [16]. Zhang (2004) presented a methodology for risk analysis and assessment of drought disasters to agricultural production in the maize-growing area of Songliao Plain of China based on geographical information systems (GIS) [17]. Liu (2010) assessed the drought risk of 13 major grain-producing provinces in China using information diffusion theory [18]. Liu (2013) used a continuous wavelet transform (CWT) to evaluate and investigate spatial patterns, temporal variations, and periodicities of dryness/wetness across Qinghai Province, Northwest China [19]. Liu (2017) examined the periodical oscillations of dryness/wetness conditions and the multi-scale relationships between dryness/wetness conditions and both the El Niño-Southern Oscillation (ENSO) and Arctic Oscillation (AO) in winter using wavelet analysis in Shaanxi of China [20].

In this study, we used R/S to analyze the trend of the agricultural drought disaster in China. Then, we quality assessed the periodic oscillation of the agricultural drought disaster at different time scales during the past 67 years from 1950 to 2016 based on the wavelet analysis. The results may provide a scientific basis for guiding agricultural production and the agricultural drought prevention work for China or other places in the world.

Historical agricultural drought disaster studies on time scales provide a very valuable basis for interpreting the present agricultural drought disaster behavior and for estimating the future tendency of the agricultural drought disaster with the climate changes. In addition, agricultural drought forecasting is helpful for establishing agricultural drought mitigation plans and for managing risks that often ensue in agricultural drought early warning monitoring and water resource systems. The specific objectives were to (a) forecast the developmental tendency of the agricultural drought disaster in the future based on the historical drought statistics by R/S, and (b) perform an analysis of the periodic oscillation of the agricultural drought disaster in China over the study period based on the wavelet analysis. All of the analyses were from the aspects of the agricultural drought disaster area, the inundated area of the agricultural drought, and the grain loss.

Data and methods are briefly described in Section 2. Analysis and results are presented in Section 3, including the trends of the agricultural drought disaster area, the inundated area of the agricultural drought disaster, and the grain loss, and the agricultural drought periodic oscillation from the aspects of the agricultural drought disaster area, the inundated area of the agricultural drought, and the grain loss. Finally, some conclusions are outlined in the final section.

2. Materials and Methods

2.1. Study Area Description

China is an agricultural country facing the natural disaster risks under the changing climate. Owing to diverse climate conditions and complicated topography influences, drought is one of the most frequent natural disasters in China and occurs with great variability at different scales. According to statistics from the Ministry of Water Resources of the People's Republic of China, there were 27 provinces (regions) that suffered an agricultural drought disaster in 2016. According to the Ministry of Civil Affairs of the People's Republic of China (<http://www.mca.gov.cn/>), the agricultural drought damage can be divided into three levels due to the crop damage. The first level is the agricultural drought disaster area, indicating that the crop damage area accounts for more than 10% of the total crop area. The second level is the agricultural drought inundated area, suggesting the crop damage area accounts for more than 30% of the total crop area. The third level is no harvest area, showing the crop damage area accounts for more than 70% of the total crop area. According to the statistics data from the Ministry of Water Resources of the People's Republic of China (<http://www.mwr.gov.cn/>), the total agricultural area affected by the drought was 2.02×10^7 ha for the year 2016, of which the agricultural drought disaster area was 9.8×10^6 ha, the inundated area of agricultural drought disaster was 6.1×10^6 ha, and no harvest area was 1.02×10^6 ha. The total crop loss was 1.9×10^{10} kg, and the crop losses due to drought in China were 13.06 billion Yuan during 2016. With the climate change continuing, agro-drought is a powerful natural force significantly shaping food security in China and the global world.

2.2. Data

The agricultural drought disaster data (1950 to 2016) used in this study was obtained from the Ministry of Water Resources of the People's Republic of China (<http://www.mwr.gov.cn/>), including the agricultural drought disaster area (ha), the agricultural drought inundated area (ha), and grain loss (kg). The data collected by the government and those data was widely used in evaluating the impact of the drought disaster.

The wavelet analysis was analyzed in MatlabR2015b software (Math Works, Natick, MA, USA, 2015). The interpolation procedure for the transformed data and the plotting of graphs were carded out using the Surfer12 plotting software (Golden Software, Golden, CO, USA, 2015). The interpolation was done using the kriging option in Surfer12, and the linear graph was done by OriginPro 2017 software (OriginProLab Corporation, Northampton, MA, USA, 2017).

2.3. Methods

2.3.1. R/S Method

We used Hurst's rescaled range (R/S) analysis and the corresponding Hurst exponent to detect the future trends of drought disasters in the study area. R/S analysis is the oldest and best-known method to estimate the Hurst exponent [21,22]. The basic idea of the R/S analytical method can be described as follows as given in the preview studies [23,24]: for the time series of a certain physical quantity ($\tau = 1, 2, \dots, n$), the average value of $x(\tau)$ is

$$x_{\tau} = \frac{1}{\tau} \sum_{t=1}^{\tau} x(t) \quad (1)$$

where the τ is the number of the time series.

The cumulative deviation is

$$X(t, \tau) = \sum_{t=1}^{\tau} (x(t) - x_{\tau}), \quad 1 \leq t \leq \tau \quad (2)$$

The expression of $X(t, \tau)$ is not only related to t but also related to τ . The difference between maximum $X(t)$ and minimum $X(t)$ at the similar τ value is denoted as

$$R(t) = \max_{1 \leq t \leq T} X(t, T) - \min_{1 \leq t \leq T} X(t, T) \quad (3)$$

The standard deviation sequence is

$$S(T) = \sqrt{\left(\frac{1}{T} \sum_{t=1}^T (x(t) - \bar{x})^2\right)} \quad (4)$$

The non-dimensional ratio R/S is defined as

$$\frac{R(T)}{S(T)} = (\alpha\Gamma)^H \quad (5)$$

H is the Hurst index, which is between 0 and 1. Based on a series of studies [26?], the following classifications of the time series can be realized: (1) $H = 0.5$ means that the sequence displays Brownian motion and the variables will not affect the future. In other words, the time series is an independent random process, indicating that the current trend will not affect the future trend. (2) $0 < H < 0.5$ indicates that the time series presents a long-term correlation, but the future overall trend is contrary to the past; it describes an anti-persistent, or a mean reverting system. Therefore, the smaller the H value, the stronger the anti-persistence. (3) $0.5 < H < 1$ describes a dynamically persistent series, or trend-reinforcing series, which means the greater the H value, the direction of the next value is more likely the same as the current value. That is to say, the process is sustainable, and the shaft additional forces variation is consistent with the previous variation, and the maintenance is stronger at higher H values.

2.3.2. The Wavelet Transform

Wavelet analysis is one of the common techniques in signals analysis because the time series does not need to be stationary compared to the fast Fourier transform (FFT) [27]. In addition, the wavelet transform can provide information about both time and frequency simultaneously at different characteristic length scales [28–30]. At present, there are a large number of wavelet transforms available for various applications [31,32], such as the haar wavelet, the Mexican-hat wavelet, Meyer and Daubechies, and the Morlet wavelet. The Morlet wavelet is a non-orthogonal complex function that keeps analysis results within a continuum. Furthermore, in the Morlet wavelet function, the selection of time scales is arbitrary [33]. In addition, providing a good balance between time and frequency localization, the Morlet wavelet is used to characterize the frequency, intensity, position of wavelet spectra peaks, and duration of variations of the stream flow series [34,35]. Therefore, we selected the Morlet wavelet to analyze the multiple time scales inherent in our data series in this study.

The Morlet wavelet analysis is a complex non-orthogonal continuous wavelet, and the basis of a Morlet wavelet (Ψ) consisting of a plane wave modulated by a Gaussian function can be defined as

$$\Psi(\eta) = \pi^{-1/4} e^{i\omega\eta - \eta^2/2} \quad (6)$$

where ω is the dimensionless frequency and η is the dimensionless time parameter. The continuous wavelet transform (CWT) has an ability to detect significant cycles and their occurrence time in the observation period. The CWT is defined as

$$w(a, b) = \frac{1}{\sqrt{a}} \int f(t) \cdot \Psi^* \left(\frac{t-b}{a} \right) dt \quad (7)$$

where a and b are scale and translation parameters, respectively, and Ψ^* is the complex conjugate of Ψ .

The wavelet variance ($W(a)$) used to detect the main periods contributing to a signal can be expressed as

$$W(a) = \frac{1}{\sqrt{a}} \int |Wx(b, a)|^2 db \quad (8)$$

Since the drought data sets used in this study are of finite length and the Morlet wavelet is not completely localized in time, errors will occur at the beginning and at the end of the wavelet power spectrum. In order to reduce the edge effects, we carried out a symmetry extension at both ends of the drought time series before undertaking the wavelet transform and then removed them.

In our study, the results of the wavelet transform will be presented in the form of four graphs as follows: the real part of wavelet coefficients, the Morlet wavelet coefficients' modulus values, the Morlet wavelet variance, and the major periodic oscillations at the different time scales. The graph of the real part of wavelet coefficients can be used to reflect the change period of different time scales and judge the changing trend on different time scales. The Morlet wavelet coefficients' modulus values graph can be used to analyze the oscillation energy of different periods. The wavelet variance graph can be used to determine the relative intensity of interference at different time scales in the signal and the main time scale. The periodic oscillation fluctuations are a reflection of the graph of the major periodic oscillations at the different time scales.

The wavelet coefficients and the variance yield of the wavelets were calculated to study the characteristics of abnormal variations. Furthermore, from the agricultural drought disaster oscillation information, we could judge the trend of the agricultural drought disasters that may occur in some area.

3. Results and Analysis

3.1. Analysis of the Hurst Index Change Trend of the Agricultural Drought Disaster

A graph is plotted for $\log(T)$ vs. $\log(R/S)$ and the slope is calculated for the study's time series, which is the Hurst index (Figure 1). As shown in Figure 1a–c, the Hurst index of the agricultural drought disaster area, inundated area of agricultural drought disaster, and grain loss was 0.821 ($R^2 = 0.99$), 0.874 ($R^2 = 0.988$), and 0.953 ($R^2 = 0.991$), respectively. All the three Hurst indexes are greater than 0.5, indicating that the process of the agricultural drought disaster had a stronger positive continuity during the study period.

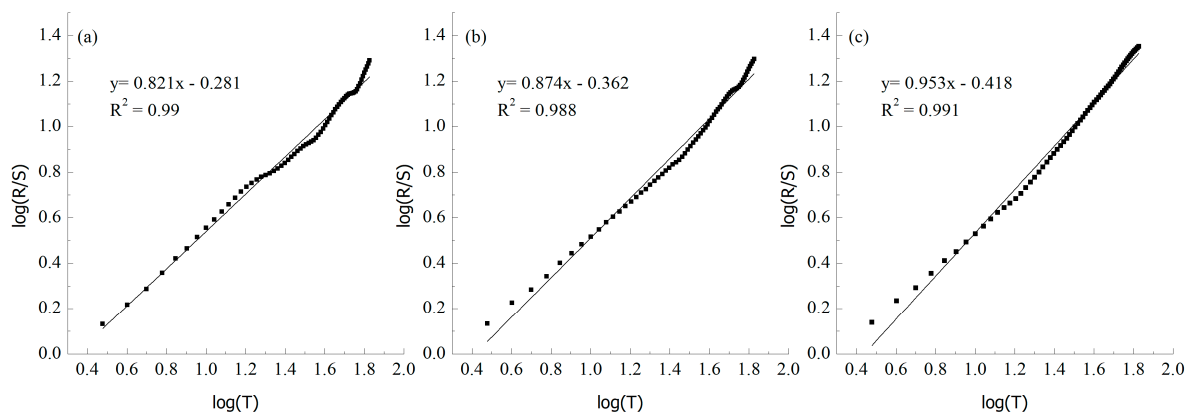


Figure 1. The change trend of the Hurst index of (a) the agricultural drought disaster area, (b) the inundated area of agricultural drought disaster, and (c) the grain loss.

As shown in Figure 2, during the study period, the annual agricultural drought disaster area (Figure 2a), inundated area of agricultural drought disaster (Figure 2b), and grain loss (Figure 2c) increased in a linear inclined rate at approximately 98.91×10^3 ha per year, 106.74×10^3 ha per year, 4.21×10^8 kg per year, respectively, indicating the overall trend of the agricultural drought increased in the past. In addition, based on Figure 1, $H > 0.5$, which means the agricultural drought process

is sustainable, and the shaft additional forces variation is consistent with the previous variation; therefore, the agricultural drought will still increase in the future. In other words, the agricultural disaster area, inundated area of agricultural drought disaster, and grain loss will still increase in the future, respectively.

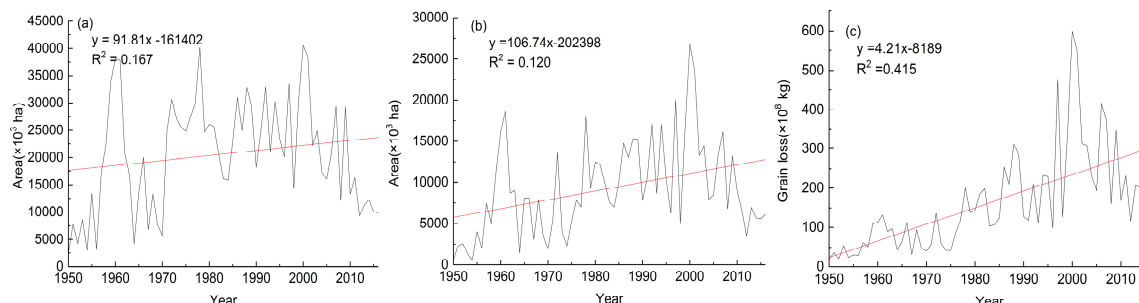


Figure 2. The annual change trend of (a) the agricultural drought disaster area, (b) the inundated area of agricultural drought disaster, and (c) the grain loss.

3.2. Analysis of the Agricultural Drought Disaster Area Variation Characteristics

Figure 3a shows the real part of the wavelet coefficients of the agricultural drought disaster area from 1950 to 2016. The solid line represents the value was above the norm, indicating the agricultural drought disaster area increased. By contrast, the dotted line indicates the value was below the norm, suggesting the agricultural drought disaster area declined. As shown in Figure 3a, there were two periodic oscillations at the scale of 6–15 years and 22–32 years. Although the conversion of the low-valued agricultural drought disaster area to high-valued agricultural drought disaster area was frequent, the periodic oscillation of 9 cycles was gentle with an overall characteristic at the scale of 6–15 years. Compared to the scale of 6–15 years, the periodic oscillation of 2 cycles was severe at the scale of 22–32 years with a local characteristic (before 1980). Until the year 2016, the contours of the agricultural drought disaster area were still not closed, indicating that an agricultural drought disaster may occur within the next few years.

The Morlet wavelet coefficients' modulus values of the agricultural drought disaster area are shown in Figure 3b for the study period. The Morlet wavelet coefficients' modulus values reflect the energy density distribution of the agricultural drought disaster area at the different time scales. Also, the coefficient modulus value represents the periodic strength of the agricultural drought disaster area. Since the larger the coefficient value of the agricultural drought disaster area, the stronger the corresponding period, and conversely, the lower the coefficient value, the weaker the corresponding period. From Figure 3b, it can be seen that the agricultural drought disaster area wavelet energy spectrum was strong at time scale of ≈ 21 –32 years, indicating the periodic oscillation was obviously at that time scale, but had a localization characteristic before 1980. Furthermore, the wavelet energy spectrum of the agricultural drought disaster area was weaker at time scale of ≈ 7 –9 years, but a more obvious cycle distribution occupied the entire study time domain (1950–2016).

As seen from the Figure 3c, the wavelet variance of the agricultural drought disaster area had four peaks, corresponding to time scales of 25 years, 15 years, 10 years, and 4 years. Figure 3d shows the two major periodic oscillations on the time scales of 10 years and 25 years. The largest peak, corresponding to the time scale of 25 years, had an average period of approximately 16 years with 4 cycles converted, indicating that the period oscillation at the time scale of 25 years fluctuated the most. Also, the second peak had approximately 8 years with 9 cycles converted at the time scale of 10 years. In summary, the agricultural drought disaster area had obvious wavelet transform period characteristics, with the short time scale change nesting in a long time scale.

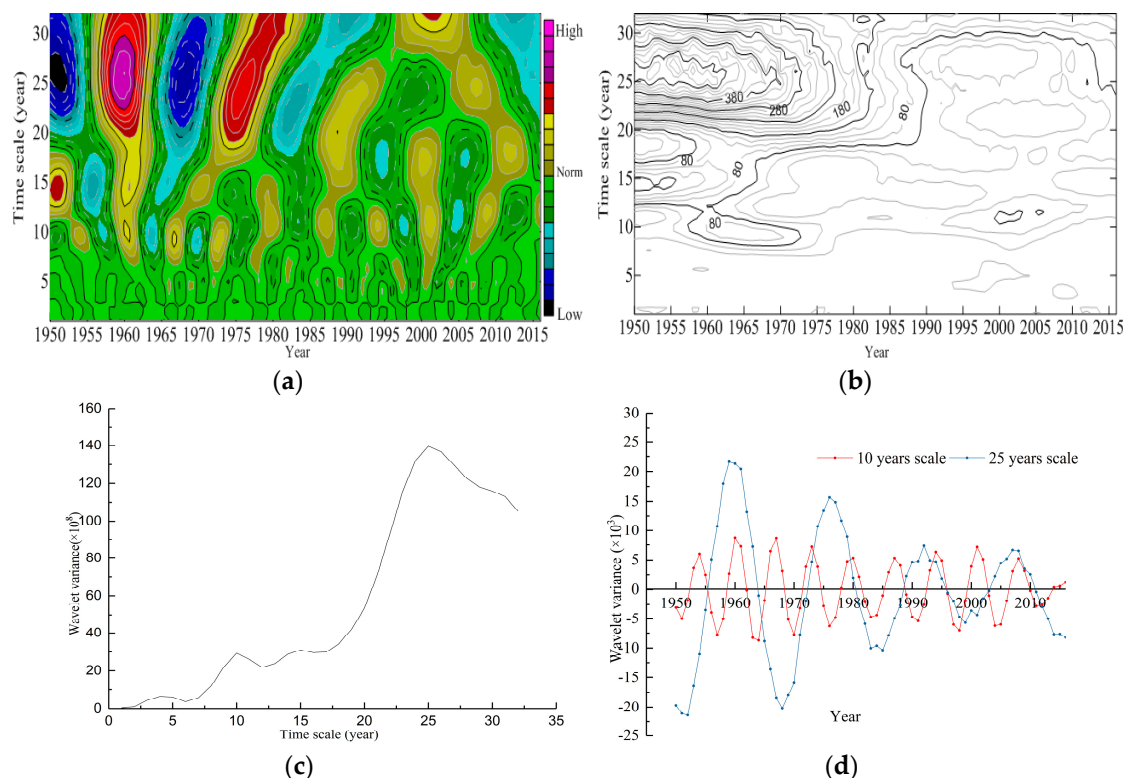


Figure 3. (a) The Morlet wavelet transforms of the agricultural drought disaster area, (b) the Morlet wavelet coefficients' modulus values of the agricultural drought disaster area, (c) the Morlet wavelet variance of the agricultural drought disaster area, and (d) the major periodic oscillations at the time scales of 10 years and 25 years.

3.3. Analysis of the Inundated Area of the Agricultural Drought Disaster Variation Characteristics

The real part of wavelet coefficients of the inundated area of the agricultural drought disaster from 1950 to 2016 is depicted in Figure 4a. The solid line represents the value was above the norm, indicating the inundated area of the agricultural drought disaster increased. In contrast, the dotted line indicates the value was below norm, suggesting the inundated area of the agricultural drought disaster declined. As shown in Figure 4a, there were two periodic oscillations at the scale of 10–18 years and 22–32 years. During the study period, the conversion of the low-valued inundated area of the agricultural drought disaster to the high-valued inundated area of the agricultural drought disaster was frequent but gentle, and it can be seen that the periodic oscillation had 7 cycles at the time scale of 10–18 years. However, at the time scale of 22–32 years, the conversion of the low-valued inundated area of the agricultural drought disaster to the high-valued inundated area of the agricultural drought disaster occurred with an overall characteristic. Meanwhile, it revealed that the next periodic oscillation will increase, according to the dotted contours of the inundated area of the agricultural drought disaster closed by 2016.

Figure 4b shows the Morlet wavelet coefficients' modulus values of the inundated area of the agricultural drought disaster during the study period. The Morlet wavelet coefficients' modulus values reflect the energy density distribution of the inundated area of the agricultural drought disaster at the different time scales. In addition, the coefficient modulus value represents the periodic strength of the inundated area of the agricultural drought disaster. The larger the coefficients value of the inundated area of the agricultural drought disaster, the stronger the corresponding period, and conversely, the smaller the coefficient value, the weaker the corresponding period. From Figure 4b, it can be seen that the inundated area of the agricultural drought disaster wavelet energy spectrum was significant at time scale of ≈ 24 –32 years, indicating the periodic oscillation was strong at that time scale, and yet it had a localization characteristic before 1980. The wavelet energy spectrum of the inundated area

of agricultural drought disaster was weaker at time scale of $\approx 4\text{--}13$ years, but a more obvious cycle distribution occupied the entire study time domain (1950–2016), which was similar with the agricultural drought disaster area.

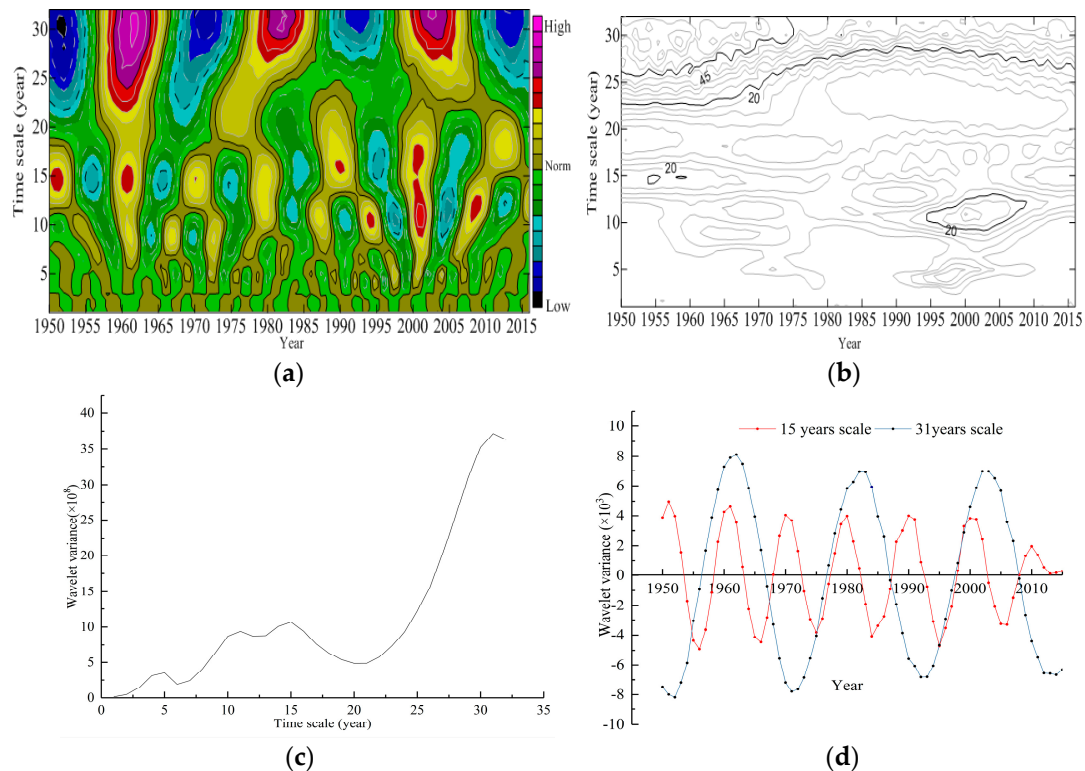


Figure 4. (a) The Morlet wavelet transforms of the inundated area of agricultural drought disaster; (b) the Morlet wavelet coefficients modulus values of the inundated area of drought disaster; (c) the Morlet wavelet variance of the inundated area of agricultural drought disaster; (d) the major periodic oscillations at the time scales of 15 years and 31 years.

We have noticed that there were still four peaks corresponding to the time scales of 31 years, 15 years, 11 years, and 5 years in Figure 4c. The largest peak corresponds to the time scale of 31 years, indicating that the period oscillation of 31 years fluctuated most; it could be considered as the first major period in the inundated area of the agricultural drought disaster change. Then, the 15-year time scale was the second major period oscillation. Figure 4d shows that the largest peak corresponding to the time scale of 31 years had the average period of approximately 20 years with 3 cycles converted, indicating that the period oscillation at the time scale of 25 years fluctuated the most. Also, the second peak had approximately 10 years with 6 cycles converted at the time scale of 15 years. In summary, the inundated area of the agricultural drought disaster also had clear wavelet transform period characteristics, with the short time scale change nesting in a long time scale.

3.4. Analysis of the Grain Loss Variation Characteristics

Figure 5a shows the real part of the wavelet coefficients of the grain loss changes from 1950 to 2016. The solid line represents the value was above the norm, indicating the grain loss increased. In contrast, the dotted line indicates the value was below the norm, suggesting the grain loss declined. As shown in Figure 5a, there were two periodic oscillations at the scale of 15–22 years and 25–32 years. During the study period, the conversion of the low-valued grain loss to the high-valued grain loss was gentle after 1985, and before 1970, there was no periodic oscillation at the time scale of 15–22 years. Furthermore, the solid contours of the grain loss closed by 2016, indicating that the next periodic oscillation will decrease at the time scale of 15–22 years. It can be seen that the periodic oscillation with

an overall characteristic had 3 cycles at the time scale of 22–32 years according to the dotted contours of the inundated area of drought disaster closing by 2016, suggesting that the next periodic oscillation will increase.

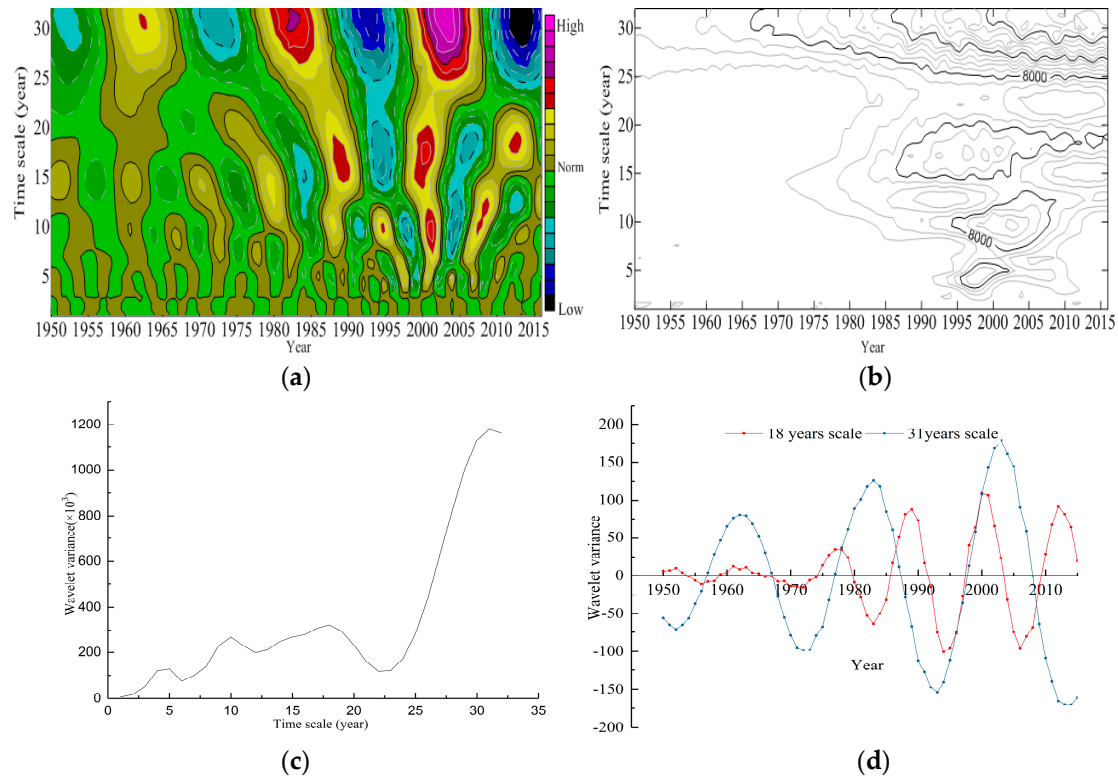


Figure 5. (a) The Morlet wavelet transforms of the grain loss, (b) the Morlet wavelet coefficients' modulus values of the grain loss, (c) the Morlet wavelet variance of the grain loss, and (d) the major periodic oscillations at the time scales of 18 years and 31 years.

The Morlet wavelet coefficients' modulus values of the grain loss are shown in Figure 5b for the study period. The Morlet wavelet coefficients' modulus values reflect the energy density distribution of the grain loss at the different time scales. Also, the coefficient modulus value represents the periodic strength of the grain loss. The larger the coefficients value of the grain loss, the stronger the corresponding period, and conversely, the smaller the coefficient value, the weaker the corresponding period. From Figure 5b, it can be seen that the grain loss wavelet energy spectrum was strong at time scale of ≈ 25 –32 years, indicating the periodic oscillation was at that time scale, but had a localization characteristic (after 1975).

As seen from Figure 5c, the wavelet variance of the grain loss had four peaks, corresponding to time scales of 31 years, 18 years, 10 years, and 4 years. Figure 5d shows the two major periodic oscillations on the time scales of 18 years and 31 years. The largest peak corresponding to the time scale of 31 years had an average period of approximately 18 years with 3 cycles converted, indicating that the period oscillation at time scale 31 years fluctuated the most. Also, the second peak had approximately 9 years with 5 cycles converted at the time scale of 18 years. In summary, the grain loss had clear wavelet transform period characteristics, with the short time scale change nesting in a long time scale.

4. Conclusions

In this study, we first predicted the future trend of the agricultural drought disaster area, the inundated area of agricultural drought disaster, and the grain loss, respectively, by R/S analysis. Then, we analyzed the characteristics of the period variation of the agricultural drought disaster area,

the inundated area of agricultural drought disaster, and the grain loss, respectively, based on the Morlet wavelet method. Some of the important conclusions derived are given below:

- (1) During the study period (1950–2016), the Hurst index of the agricultural disaster area, the inundated area of agricultural drought disaster and the grain loss was 0.821, 0.874, and 0.953, respectively, indicating the agricultural drought disaster had a long-enduring characteristic in China. Since the overall trend of the agricultural drought increased in the past, it will still increase in the future.
- (2) According to the results of the Morlet analysis of the agricultural disaster area and the inundated area of agricultural drought disaster, we noticed that the time series of the agricultural drought had multiple time scale features. That is to say, the periodic variation on a large scale contained periodic variation on a small scale.
- (3) In the last 67 years, the strong wavelet energy spectrum of the agricultural disaster area, the inundated area of agricultural drought disaster, and the grain loss had an average period of approximately 16 years, 16 years, and 18 years, respectively. Furthermore, the cycle changes of the agricultural drought disaster area and the inundated area of the agricultural drought disaster had a localization characteristic before 1980, while the cycle changes of the grain loss had a localization characteristic after 1975.
- (4) According to the results, it was concluded that wavelet analysis can be a useful method to analyze detailed temporal patterns of agricultural drought disaster over different temporal scales. Furthermore, in our study, we only forecasted the trend of the agricultural drought disaster, and as a future work, we will use the model for forecasting the level of drought disaster in subsequent years. In addition, in this study we took the whole of China as an example; however, China has a complex climate and different plants, and as such, in a future study we will study the agricultural drought disaster at the provincial scale.

Author Contributions: Formal analysis, Q.W., L.T. and W.Z.; Funding acquisition, J.L.; Software, Q.W., L.T. and X.L.; Writing—original draft, Q.W. and Y.L.; Writing—review & editing, Q.W. and J.L. All authors have approved the final article.

Funding: This research was funded by National key Research and Development project (2018YFD0800201), the APN Global Change Fund Project (No. ARCP2015-03CMY-Li & CAF2015-RR14-NMY-Odeh), the Jiangsu Province Agricultural Three Renovations Project of China (No. SXGC [2014]287), The National Natural Science Foundation of China (No. 41271361), The Key Project of Chinese National Programs for Fundamental Research and Development (973 Program, No. 2010CB950702), The National High Technology Project (863 Plan, No. 2007AA10Z231), The National Natural Science Foundation (41501575) and the Public Sector Linkages Program supported by the Australian Agency for International Development (PSLP: No. 64828).

Acknowledgments: We are grateful to the editor and anonymous reviewers.

Conflicts of Interest: The authors declare no conflict of interest.

References

1. Homdee, T.; Pongput, K.; Kanae, S. A comparative performance analysis of three standardized climatic drought indices in the chi river basin, Thailand. *Agric. Nat. Resour.* **2016**, *50*, 211–219. [[CrossRef](#)]
2. Glantz, M.H. Understanding: The drought phenomenon: The role of definitions. *Water Int.* **1985**, *10*, 111–120.
3. Heim, R.R.J. A review of twentieth-century drought indices used in the United States. *Bull. Am. Meteorol. Soc.* **2002**, *83*, 1149–1165. [[CrossRef](#)]
4. Wang, J.S. Progress and prospect on drought indices research. *Arid Land Geogr.* **2007**, *1*, 12.
5. Wu, Z.; Mao, Y.; Li, X.; Lu, G.; Lin, Q.; Xu, H. Exploring spatiotemporal relationships among meteorological, agricultural, and hydrological droughts in southwest china. *Stoch. Environ. Res. Risk Assess.* **2015**, *30*, 1–12. [[CrossRef](#)]
6. Bao, G.; Liu, Y.; Liu, N.; Linderholm, H.W. Drought variability in eastern Mongolian plateau and its linkages to the large-scale climate forcing. *Clim. Dyn.* **2015**, *44*, 717–733. [[CrossRef](#)]

7. Wang, Q.; Wu, J.; Lei, T.; He, B.; Wu, Z.; Liu, M.; Mo, X.; Geng, G.; Li, X.; Zhou, H. Temporal-spatial characteristics of severe drought events and their impact on agriculture on a global scale. *Quat. Int.* **2014**, *349*, 10–21. [[CrossRef](#)]
8. Guo, H. Spatial and temporal characteristics of droughts in central Asia during 1966–2015. *Sci. Total Environ.* **2018**, *624*, 1523–1538. [[CrossRef](#)] [[PubMed](#)]
9. Zhao, G.; Zhou, G.; Wang, J. Application of r/s method for dynamic analysis of additional strain and fracture warning in shaft lining. *J. Sens.* **2015**, *2015*, 1–7.
10. Mandelbrot, B.B. *The Fractal Geometry of Nature*; Birkhauser Verlag: Basel, Switzerland, 1983; p. 468.
11. Polikar, R. The Story of Wavelets. Available online: <https://pdfs.semanticscholar.org/6ec3/e93c0f3bb0a0c653ab4091edc68a8780d037.pdf> (accessed on 18 May 2018).
12. July, F. Drought risk assessment in Yunnan province of china based on wavelet analysis. *Adv. Meteorol.* **2015**, *2016*, 1–10.
13. Peng, J.; Liu, Z.; Liu, Y.; Wu, J.; Han, Y. Trend analysis of vegetation dynamics in Qinghai–Tibet plateau using hurst exponent. *Ecol. Indic.* **2012**, *14*, 28–39. [[CrossRef](#)]
14. Serban, C.; Maftei, C. Evaluation of hurst exponent for precipitation time series. In Proceedings of the Wseas International Conference on Computers, Corfu Island, Greece, 23–25 July 2010; Volume 2, pp. 590–595.
15. Huang, R.; Yong, L.; Lin, W. Analyses of the causes of severe drought occurring in southwest china from the fall of 2009 to the spring of 2010. *Chin. J. Atmos. Sci.* **2012**, *36*, 443–457.
16. Li, S.K.; Huo, Z.G.; Wang, S.Y.; Liu, R.H.; Sheng, S.X.; Liu, J.L.; Ma, S.Q.; Xue, C.Y. Risk evaluation system and models of agrometeorological disasters. *J. Nat. Disasters* **2004**, *13*, 77–87.
17. Zhang, J. Risk assessment of drought disaster in the maize-growing region of Song Liao plain, China. *Agric. Ecosyst. Environ.* **2004**, *102*, 133–153. [[CrossRef](#)]
18. Liu, Y.B.; Liu, L.M.; Xu, D.; Zhang, S.H. Risk assessment of flood and drought in major grain-producing areas based on information diffusion theory. *Trans. Chin. Soc. Agric. Eng.* **2010**, *26*, 1–7.
19. Liu, Z.; Zhou, P.; Zhang, F.; Liu, X.; Chen, G. Spatiotemporal characteristics of dryness/wetness conditions across Qinghai province, northwest China. *Agric. For. Meteorol.* **2013**, *182–183*, 101–108. [[CrossRef](#)]
20. Liu, Z.; Zhang, X.; Fang, R. Multi-scale linkages of winter drought variability to enso and the arctic oscillation: A case study in Shaanxi, north China. *Atmos. Res.* **2017**, *200*, 117–125. [[CrossRef](#)]
21. Granero, M.A.S.; Segovia, J.E.T.; Pérez, J.G. Some comments on hurst exponent and the long memory processes on capital markets. *Phys. A Stat. Mech. Appl.* **2012**, *387*, 5543–5551. [[CrossRef](#)]
22. Hurst, H.E. Long term storage capacity of reservoirs. *Trans. Am. Soc. Civ. Eng.* **1951**, *116*, 776–808.
23. Wang, X.L.; Hu, B.Q.; Xia, J. R/s analysis method of trend and aberrance point on hydrological time series. *J. Wuhan Univ. Hydraul. Electr. Eng.* **2002**, *35*, 10–12.
24. Yu, Y.; Chen, X.W. Analysis of future trend characteristics of hydrological time series based on r/s and mann-kendall methods. *J. Water Resour. Water Eng.* **2008**, *9*, 41–44.
25. Shi, P.; Wu, M.; Qu, S.; Jiang, P.; Qiao, X.; Chen, X.; Zhou, M.; Zhang, Z. Spatial distribution and temporal trends in precipitation concentration indices for the southwest china. *Water Resour. Manag.* **2015**, *29*, 3941–3955. [[CrossRef](#)]
26. Zhao, G.S.; Zhou, G.Q.; Zhao, X.D.; Wei, Y.Z.; Li, L.J. R/s analysis for stress evolution in shaft lining and fracture prediction method. *Adv. Mater. Res.* **2012**, *374–377*, 2271–2274. [[CrossRef](#)]
27. Piotrkowski, R.; Gallego, A.; Castro, E.; García-Hernandez, M.T.; Ruzzante, J.E. Ti and cr nitride coating/steel adherence assessed by acoustic emission wavelet analysis. *NDT E Int. J.* **2005**, *38*, 260–267. [[CrossRef](#)]
28. D’Attellis, C.E.; Fernández-Berdaguer, E.M. *Wavelet Theory and Harmonic Analysis in Applied Sciences*; Birkhauser: Basel, Switzerland, 1997; pp. 3–13.
29. Daubechies, I. Ten lectures on wavelets. *CBMS-NSF Ser. Appl. Math. SIAM* **1995**, *6*, 1671.
30. RonnieSircar. An introduction to wavelets and other filtering methods in finance and economics. *Waves Random Med.* **2001**, *12*, 399.
31. Nakken, M. Wavelet analysis of rainfall–runoff variability isolating climatic from anthropogenic patterns. *Environ. Model. Softw.* **1999**, *14*, 283–295. [[CrossRef](#)]
32. Issartel, J.; Marin, L.; Gaillot, P.; Bardainne, T.; Cadopi, M. A practical guide to time-frequency analysis in the study of human motor behavior: The contribution of wavelet transform. *J. Mot. Behav.* **2006**, *38*, 139–159. [[CrossRef](#)] [[PubMed](#)]

33. Zhang, Q.; Lu, W.; Chen, S.; Liang, X. Using multifractal and wavelet analyses to determine drought characteristics: A case study of Jilin province, China. *Theor. Appl. Climatol.* **2016**, *125*, 829–840. [[CrossRef](#)]
34. Liu, D.; Liu, X.; Li, B.; Zhao, S.; Li, X. Multiple time scale analysis of river runoff using wavelet transform for Dagujia river basin, Yantai, China. *Chin. Geogr. Sci.* **2009**, *19*, 158–167. [[CrossRef](#)]
35. Yang, C.; Yu, Z.; Hao, Z.; Zhang, J.; Zhu, J. Impact of climate change on flood and drought events in huaihe river basin, china. *Hydrol. Res.* **2012**, *43*, 14–22. [[CrossRef](#)]



© 2018 by the authors. Licensee MDPI, Basel, Switzerland. This article is an open access article distributed under the terms and conditions of the Creative Commons Attribution (CC BY) license (<http://creativecommons.org/licenses/by/4.0/>).